Available online at www.sciencedirect.com
SciVerse ScienceDirect
Ceramics International 39 (2013) 5321–5325
CERAMICS INTERNATIONAL
www.elsevier.com/locate/ceramint

Formation and characterization of flame synthesized hexagonal zinc oxide nanorods for gas sensor applications

P. Kathirvel[a,1], J. Chandrasekaran[b,*], D. Manoharan[b], S. Kumar[c]

[a]Research and Development Centre, Bharathiar University, Coimbatore 641046, Tamil Nadu, India
[b]Department of Physics, Sri Ramakrishna Mission Vidyalaya College of Arts and Science, Coimbatore 641020, Tamil Nadu, India
[c]Centre for Engineered Coatings, International Advance Research Centre for Power Metallurgy and New Materials (ARCI), Hyderabad 500005, Andhra Pradesh, India

Received 11 October 2012; received in revised form 11 December 2012; accepted 12 December 2012
Available online 4 January 2013

Abstract

Highly crystalline ZnO nanorods were synthesized via a simple flame synthesis technique from micro-metallic Zn. The X-ray diffraction analysis confirms presence of zinc oxide nanorods with highly oriented wurtzite structure in which the oxygen atoms are arranged in a hexagonal close packed lattice and zinc atoms occupy half of the tetrahedral sites. The photoluminescence spectrum of the nanorods shows the presence of interstitial vacancy of Zn. Energy dispersive X-ray spectrum reveals oxygen deficiency, which leads to ferromagnetic behavior and gas sensing property of the nanorods.

Keywords: A. Gas phase reaction; C. Optical properties; D. ZnO; E. Sensors

1. Introduction

In the last few decades, the study of multifunctional materials has had a leading edge in nanoscience and nanotechnology. Zinc oxide (ZnO) is a wide band-gap (3.37 eV) compound semiconductor that is suitable for short wavelength optoelectronic applications. It is a versatile functional material that has a diverse group of growth morphologies, such as nanocombs, nanorings, nanohelixes/nanosprings, nanobelts, nanorods and nanocages [1]. The most effective functional materials for photocatalytic applications are nanosized semiconductor oxides. Intensive research has focused on fabricating ZnO nanostructures and correlating their morphologies with their size-related optical and electrical properties [2]. ZnO nanostructures have been identified as nanorods, nanowires, nanobelts, nanotubes, nanobridges, nanohelixes, etc. Among the nanostructures, ZnO nanorods and nanowires are mostly studied because of their easy nanomaterials formation and device applications [3]. Several deposition techniques have been employed for the synthesis of zinc oxide nanostructures such as physical evaporation, hydrothermal, chemical vapor deposition, etc. [4–7]. In addition to these techniques, the flame synthesis method is a prominent and most effective process because it offers many advantages with excellent control over stoichiometry with inexpensive equipment. Multifunctional ZnO nanomaterials play an important role in the solid state gas sensors owing to their high surface to volume ratio. ZnO nanowires have already been studied and found to have high sensitivity with a fast response time of 10 s for ethanol gas. The present study deals with the growth of ZnO nanorods, and their structural, luminescence, magnetic, thermal and gas-sensing characteristics with a fast response and recovery time of 23 s and 35 s respectively.

2. Experimental

The experimental setup consists of oxygen and acetylene cylinders as shown in Fig. 1. A horizontal nozzle is fitted so that the metallic zinc from the feeder falls vertically into

*Corresponding author. Tel.: +91 422 2692461; fax: +91 422 2692676.
E-mail address: jchandaravind@yahoo.com (J. Chandrasekaran).
[1]Present address: Department of Physics, United Institute of Technology, Coimbatore 641020, Tamil Nadu, India.

0272-8842/$ - see front matter
http://dx.doi.org/10.1016/j.ceramint.2012.12.037

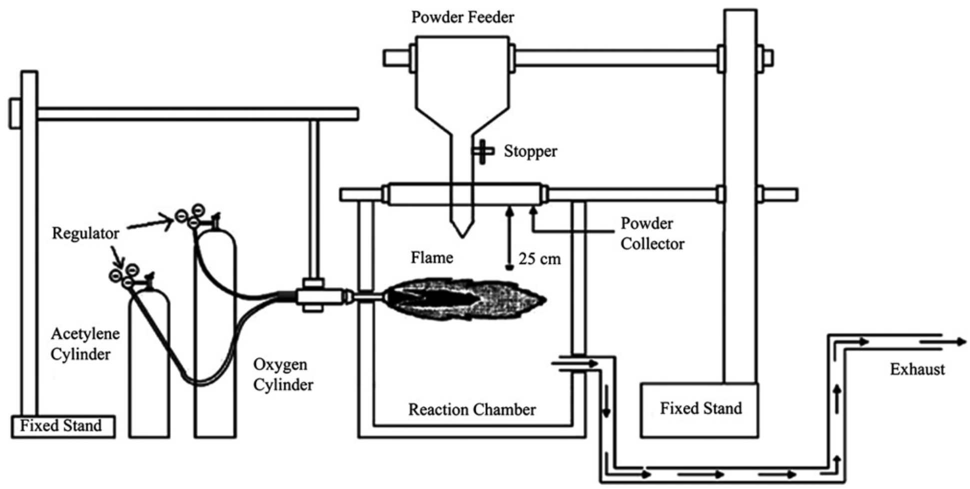

Fig. 1. Experimental setup of flame synthesis technique.

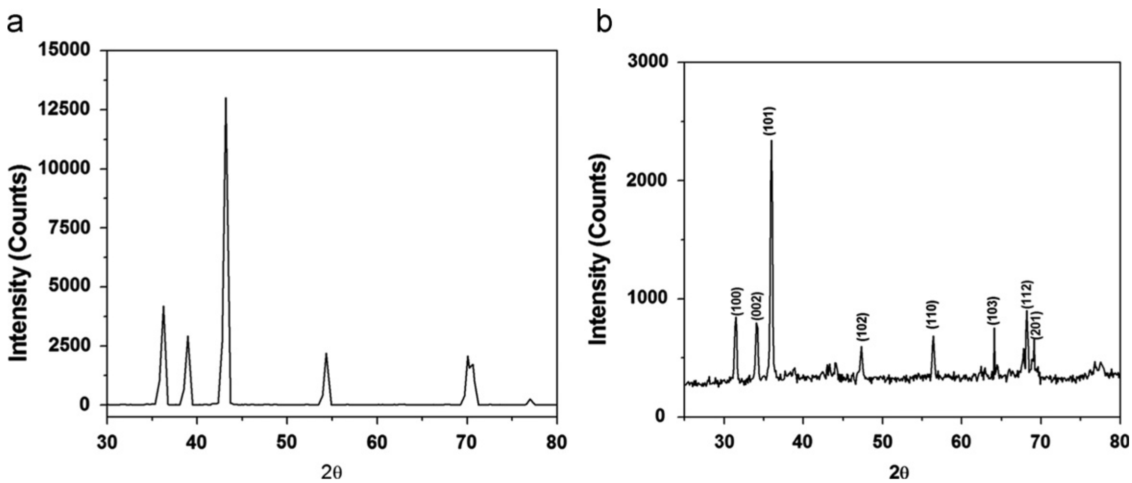

Fig. 2. XRD pattern of (a) metallic zinc and (b) ZnO nanorods.

the flame emanating from the nozzle. A powder collector plate was placed at a distance of 25 cm above the flame. Metallic zinc is fed into the flame, which contains $50O_2$:$50C_2H_2$. The particles melt and react with the flame oxygen, resulting in the deposition of zinc oxide on the surface of the powder collector.

3. Characterization

The synthesized nanorods are characterized by X-ray diffraction to find out the resultant phases with an X-ray diffraction (XRD) model Siemens D5000 with Cu Kα radiation ($\lambda = 1.\ 5406$ Å and $\theta = 30$–$80°$). The shape of the nanorods is examined using a FEI Quanta FEG 200 High Resolution Scanning Electron Microscope (HRSEM). Thermal transformations of the zinc oxide nanorods are recorded by thermogravimetric analysis (TGA, Netsch STA 409 Selb, Germany). The particle size distribution of the nanorods was observed by using a laser particle size analyzer, Fritsch model analysette 22 compact, Idar-Obestein, Germany. The surface defects and the transition mechanism are investigated by photoluminescence (PL) study using a Fluorescence Spectrophotometer AE-F96PRO. The magnetic behavior of the nanorods is traced using Lakeshore VSM 7410.

4. Discussion

The phase and crystallographic orientation of metallic zinc (Zn) and zinc oxide (ZnO) nanorods are identified by X-ray diffraction analysis as shown in Fig. 2(a) and (b) respectively. The position of the peaks corresponding to (100), (002), (101), (102), (110), (103), (200), (112), (201), and (202) confirms the formation of zinc oxide nanorods with highly oriented wurtzite structure in which the oxygen atoms are arranged in a hexagonal close packed lattice and zinc atoms occupy half the tetrahedral sites. The result matches JCPDS card number 36-1451 of the zinc oxide nanostructure [8]. The lattice constants of the nanaorods are measured to be $a = 0.3249$ nm and $c = 0.5212$ nm, which are in good agreement with the values of the bulk wurtzite ZnO. The sharp and high intensity peaks show the high crystalline nature of the zinc oxide nanorods [9]. No impurity phase can be detected within the limit of XRD measurement. The energy dispersive X-ray spectrum (EDAX) of the synthesized ZnO nanorods shows the absence of impurities and the presence of oxygen vacancies shown in Fig. 3.

The room temperature photoluminescence spectrum of the zinc oxide nanorods with an irradiating wavelength of 370 nm is shown in Fig. 4. It shows blue emission at 471 nm and green emission at 546 nm in the visible region. The intensity of visible emission is higher than that of the excitation wavelength owing to increased defect density [10]. The transition due to oxygen anticipated vacancy defect is responsible for the blue emission. The interstitial Zn and O centers, which are responsible for the recombination of shallow trapped electrons with a deeply trapped hole, lead to the green emission at 546 nm [11–15]. The defects in the metal oxides result in chemical absorption and a large amount of vacancies enhance the gas sensing property.

From the scanning electron micrograph of the micro-zinc (Zn) shown in Fig. 5, it is evident that the size of the particles ranges from 40 μm to 50 μm and is found to be irregular in shape. The zinc oxide (ZnO) nanorods have been identified by the high resolution scanning electron microscopy shown in Fig. 6. It is evident that the rods have a highly oriented hexagonal structure and the diameter of the rods ranges from 31.7 nm to 53.5 nm. It is also found that the neck to neck formation of the nanorods is a very rare phenomenon in nanostructures, especially in nanorods and nanowires. During the final stage of growth the adjacent nanoparticles contact each other within a chain forming a neck and the mass redistribution eliminates the

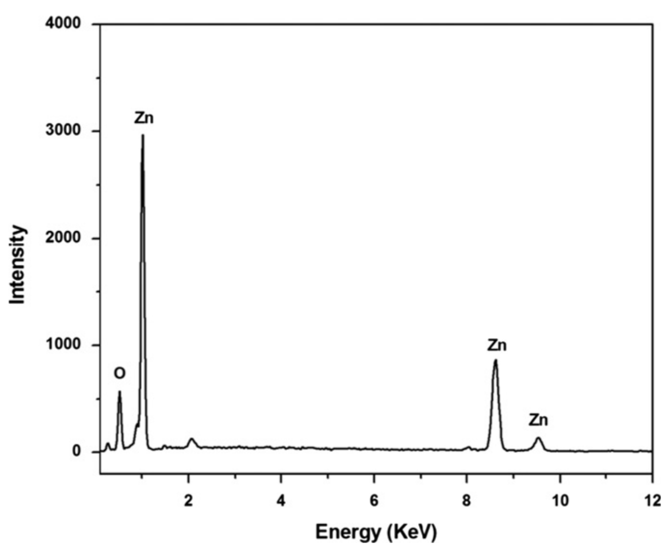

Fig. 3. EDAX spectra of ZnO nanorods.

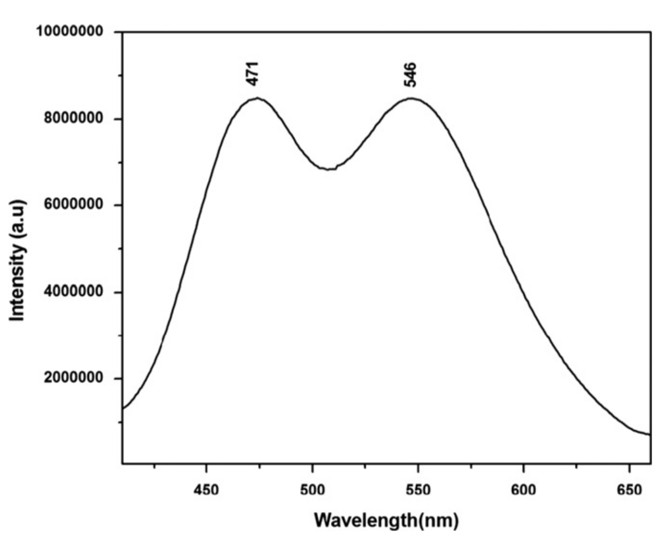

Fig. 4. PL spectra of ZnO nanorods.

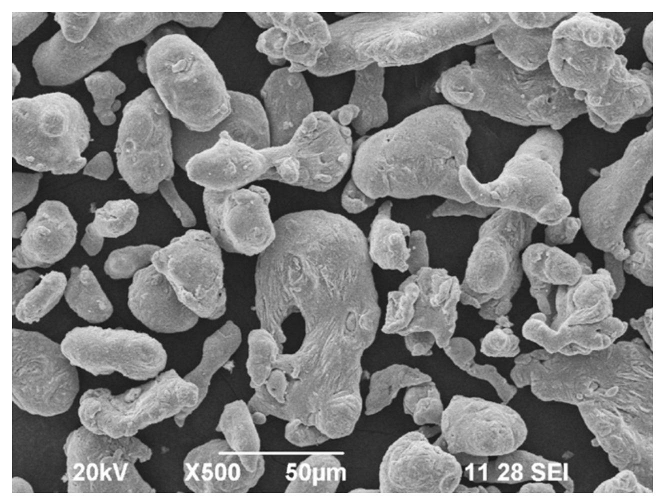

Fig. 5. SEM image of metallic zinc.

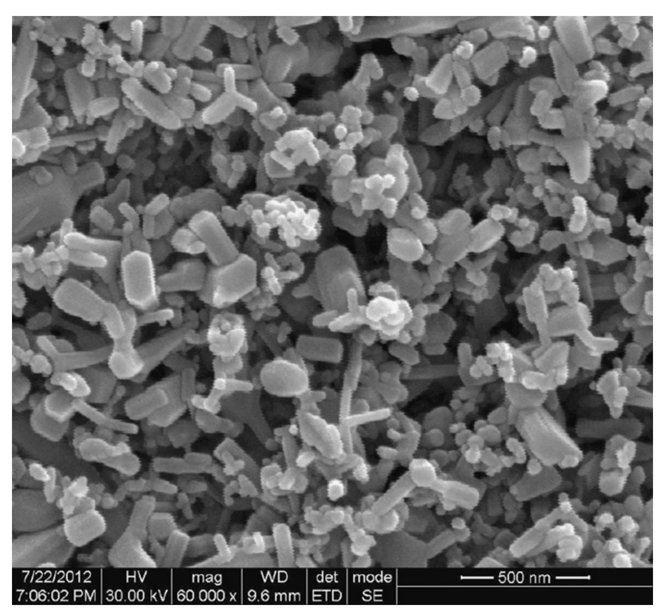

Fig. 6. HRSEM image of ZnO nanorods.

neck and forms nanowires [16]. A polycrystalline nanowire straightens and transforms into single crystal nanorods with a well defined shape or structure. The particle size analysis shown in Fig. 7 proves that the size of zinc oxide nanorods ranges from 35 nm to 55 nm and it also matches with the size of the nanorods measured from high resolution electron microscopy.

The magnetic hysteresis (*M–H* Curve) of the synthesized zinc oxide nanorods recorded at 300 K is shown in Fig. 8. The ZnO nanorods exhibit ferromagnetic behavior. The coercivity field is 445.27 G at an applied field of 19.50×10^3 G. It is reported that the singly ionized oxygen vacancy is responsible for the ferromagnetism in the ZnO nanorods. According to theoretical investigations the interstitial zinc vacancy defect only leads to the ferromagnetism in the ZnO nanorods [17]. The presence of the zinc vacancy defect is also confirmed by the photoluminescence study of the ZnO nanorods, which indicates green emission in the visible region.

The thermogravimetric analysis (TGA) is used to determine the composition of the materials and their thermal stability at temperatures up to 550 °C shown in Fig. 9. It is found that the weight loss from 0 °C to 150 °C is due to water of hydration. The second weight loss is due to the decomposition of chemically bound groups between 150 °C and 350 °C [18]. The third weight loss from 350 °C to 550 °C is due to the decomposition of the impurity ions from ZnO lattice and the new phase formation of ZnO nanorods. This is also confirmed by the presence of sharp peaks in the X-ray diffraction analysis [9].

The gas sensing performance of the ZnO nanorods at 300 K is studied and shown in Fig. 10. The gas sensing response of the ZnO rods is tested for H_2S from the concentration of 50 ppm to 250 ppm. The gas sensing response (S) is defined as $S=100[R_a-R_g]/R_a$, where R_a is the resistance of the nanorod sensor in air and R_g is the resistance of the nanorod sensor in the test gas [19]. From

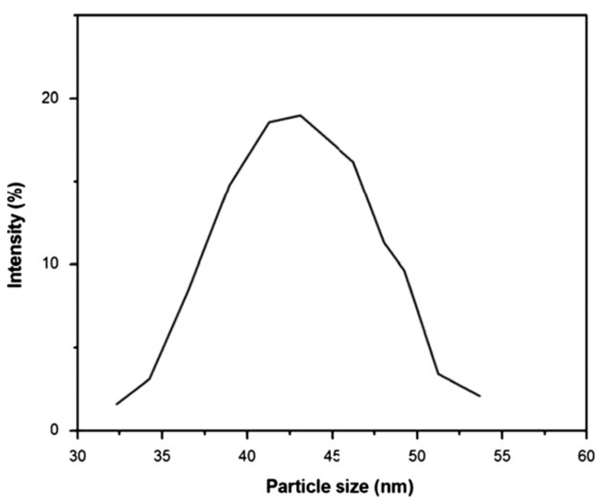

Fig. 7. Particle size analysis of ZnO nanorods.

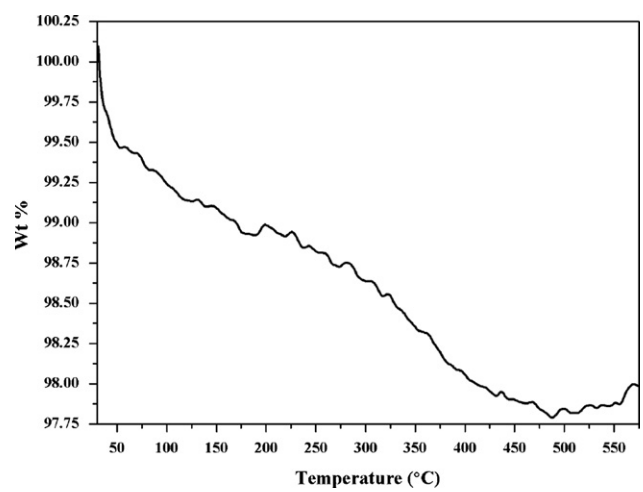

Fig. 9. TGA spectra of ZnO nanorods.

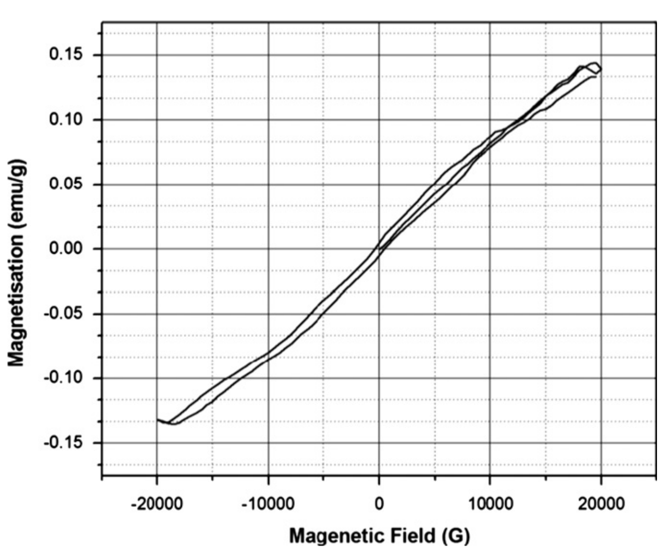

Fig. 8. Hysteresis curve of ZnO nanorods.

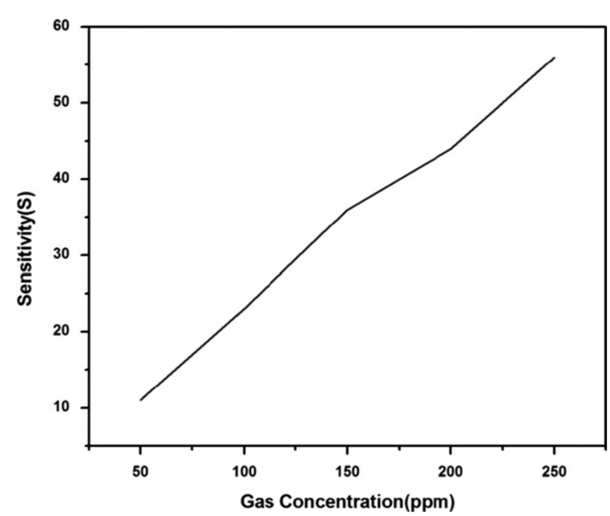

Fig. 10. Gas sensing response of ZnO nanorods.

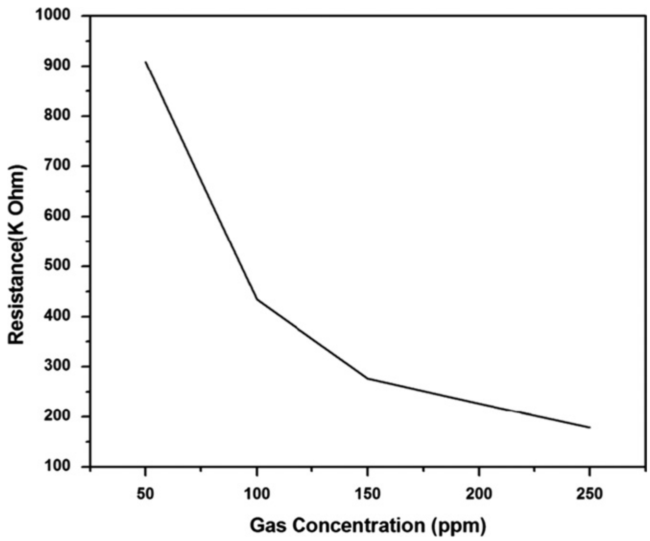

Fig. 11. Resistance vs gas concentration of ZnO nanorods.

the gas sensing response it is clear that the sensitivity increases from 11 to 56 as the gas concentration increases from 50 ppm to 250 ppm. In the metal oxide semiconductor sensor the change in resistance is due to the adsorption and desorption of oxygen on the surface of the sensing materials shown in Fig. 11. The linear graph of the gas response also suggests a large number of oxygen vacancies in the ZnO nanorods [10]. The response time (T_{res}) and recovery time (T_{rec}) are defined as the time taken for 90% of the variation in resistance upon exposure to gas and to air and are found to be 23 s and 35 s respectively.

5. Conclusions

High crystalline and hexagonal closely packed ZnO nanorods have been grown successfully by a simple flame synthesis technique. The energy dispersive X-ray analysis confirms the absence of impurities. It is found that the nanorods exhibit ferromagnetism at 300 K owing to the interstitial Zn center and the recombination of a shallow trapped electron with a deeply trapped hole. Our results exhibit enhanced gas sensitivity of the nanorods and the diameter of the nanorods can be controlled by employing suitable optimization/synthesis parameters.

References

[1] Zhong Lin Wang., Zinc oxide nanostructures: growth, properties and applications, Journal of Physics: Condensed Matter 16 (2004) R829–R858.

[2] A. Umar, S. Lee, Y.S. Lee, K.S. Nahm, Y.B. Hahn, Star-shaped zinc oxide (ZnO) nanostructures on silicon by cyclic feeding chemical vapor deposition, Journal of Crystal Growth 277 (2005) 479–484.

[3] Gianni Ciofani, Giada Graziana Genchi, Virgilio Mattoli, ZnO nanowire arrays as substrates for cell proliferation and differentiation, Materials Science and Engineering 32 (2012) 341–347.

[4] S.Y. Li, C.Y. Lee, T.Y. Tseng, Copper-catalyzed ZnO nanowires on silicon (1 0 0) grown by vapor–liquid–solid process, Journal of Crystal Growth 247 (2003) 357–362.

[5] Zheng Wei Pan, Zu Rong Dai, Zhong Lin Wang, Nanobelts of semiconducting oxides, Science 291 (2001) 1947–1949.

[6] J.Y. Lao, J.Y. Huang, D.Z. Wang, Z.F. Ren, ZnO nanobridges and nanonails, Nano Letters 3 (2003) 235–238.

[7] Chunrui Wang Gyu-Chul Yi, Won Il Park, ZnO nanorods: synthesis, characterization and applications, Semiconductor Science and Technology 20 (2005) S22–S33.

[8] A. Saleh, M.A. Gondal, Q.A. Drmosh, Z.H. Yamani, A. Al-Yamani, Enhancement in photocatalytic activity for acetaldehyde removal by embedding ZnO nanoparticles on multiwall carbon nanotubes, Chemical Engineering Journal 166 (2011) 407–412.

[9] Tapas Kumar Kundu, Nantu Karak, Puspendu Barik, Satyajit Saha, Optical properties of ZnO nanoparticles prepared by chemical method using poly(VinylAlcohol) (PVA) as capping agent, International Journal on Soft Computing 1 (2011) 19–24.

[10] D.C. Reynolds, D.C. Look, B. Jogai, H. Morkoc, Similarities in the bandedge and deep-centre photoluminescence mechanisms of ZnO and GaN, Solid State Communications 101 (1997) 643–646.

[11] A.F. Kohan, G. Ceder, D. Morgan, G. Chris, Van de Walle, First-principles study of native point defects in ZnO, Physical Review B 61 (2000) 15019–15027.

[12] F.A. Kroger, H.J. Vink, The origin of the fluorescence in self activated ZnS, CdS, and ZnO, Journal of Chemical Physics 22 (1954) 250–252.

[13] M. Liu, A.H. Kitai, P. Mascher, Point defects and luminescence centres in zinc oxide and zinc oxide doped with manganese, Journal of Luminescence 54 (1992) 35–42.

[14] D. Li, Y.H. Leung, A.B. Djurisic, Z.T. Liu, M.H. Xie, S.L. Shi, S.J. Xu, W.K. Chan, Different origins of visible luminescence in ZnO nanostructures fabricated by the chemical and evaporation methods, Applied Physics Letters 85 (2004) 1601–1603.

[15] Hong-Gang Liao, Likun Cui, Stephen Whitelam, Haimei Zheng, Real-time imaging of Pt_3Fe nanorod growth in solution, Science 336 (2012) 1011–1014.

[16] Xiaohu Huang, Guanghai Li, Lei Duan, Liang Li, Xincun Doua, Lide Zhang, Formation of ZnO nanosheets with room-temperature ferromagnetism by co-doping with Mn and Ni, Scripta Materialia 60 (2009) 984–987.

[17] G. Murugadoss, Synthesis and characterization of transition metals doped ZnO nanorods, Journal of Materials Science and Technology 28 (2012) 587–593.

[18] Wei Ang, Wang Zhao, Pan Liu-Hua, Li Wei-Wei Xiong Li, Dong Xiao-Chen, Huang Wei, Room-temperature NH_3 gas sensor based on hydrothermally grown ZnO nanorods, Chinese Physics Letters 28 (2011) 080702-1–080702-4.

[19] S.K. Gupta, Aditee Joshi, Manmeet Kaur, Development of gas sensors using ZnO nanostructures, Journal of Chemical Sciences 122 (2010) 57–62.